# Tiling Path Genomic Profiling of Grade 3 Invasive Ductal Breast Cancers

Rachael Natrajan,[1] Maryou B. Lambros,[1] Socorro María Rodríguez-Pinilla,[3] Gema Moreno-Bueno,[4] David S.P. Tan,[1] Caterina Marchió,[1] Radost Vatcheva,[1] Sydonia Rayter,[1] Betania Mahler-Araujo,[1] Laura G. Fulford,[2] Daniela Hungermann,[6] Alan Mackay,[1] Anita Grigoriadis,[2] Kerry Fenwick,[1] Narinder Tamber,[1] David Hardisson,[5] Andrew Tutt,[1] Jose Palacios,[7] Christopher J. Lord,[1] Horst Buerger,[8] Alan Ashworth,[1] and Jorge S. Reis-Filho[1]

**Abstract**

**Purpose:** To characterize the molecular genetic profiles of grade 3 invasive ductal carcinomas of no special type using high-resolution microarray-based comparative genomic hybridization (aCGH) and to identify recurrent amplicons harboring putative therapeutic targets associated with luminal, HER-2, and basal-like tumor phenotypes.

**Experimental Design:** Ninety-five grade 3 invasive ductal carcinomas of no special type were classified into luminal, HER-2, and basal-like subgroups using a previously validated immunohistochemical panel. Tumor samples were microdissected and subjected to aCGH using a tiling path 32K BAC array platform. Selected regions of recurrent amplification were validated by means of *in situ* hybridization. Expression of genes pertaining to selected amplicons was investigated using quantitative real-time PCR and gene silencing was done using previously validated short hairpin RNA constructs.

**Results:** We show that basal-like and HER-2 tumors are characterized by "sawtooth" and "firestorm" genetic patterns, respectively, whereas luminal cancers were more heterogeneous. Apart from confirming known amplifications associated with basal-like (1q21, 10p, and 12p), luminal (8p12, 11q13, and 11q14), and HER-2 (17q12) cancers, we identified previously unreported recurrent amplifications associated with each molecular subgroup: 19q12 in basal-like, 1q32.1 in luminal, and 14q12 in HER-2 cancers. *PPM1D* gene amplification (17q23.2) was found in 20% and 8% of HER-2 and luminal cancers, respectively. Silencing of PPM1D by short hairpin RNA resulted in selective loss of viability in tumor cell lines harboring the 17q23.2 amplification.

**Conclusions:** Our results show the power of aCGH analysis in unraveling the genetic profiles of specific subgroups of cancer and for the identification of novel therapeutic targets.

**Authors' Affiliations:** [1]The Breakthrough Breast Cancer Research Centre, Institute of Cancer Research; [2]The Ludwig Institute for Cancer Research, London, United Kingdom; [3]Centro Nacional de Investigaciones Oncológicas; [4]Departamento de Bioquímica, Instituto de Investigaciones Biomédicas "Alberto Sols" Consejo Superior de Investigaciones Científicas, Universidad Autónoma de Madrid; [5]Department of Pathology, Hospital Universitario La Paz, Madrid, Spain; [6]Institute of Pathology, Muenster University Hospital, Muenster, Germany; [7]Servicio de Anatomia Patologica, Hospital Virgen del Rocío, Seville, Spain; and [8]Institute of Pathology, Paderborn, Germany

Received 7/19/08; revised 11/4/08; accepted 12/8/08; published OnlineFirst 3/24/09.

**Grant support:** Breakthrough Breast Cancer; Associazione Italiana per la Ricerca sul Cancro regional grant 1182 (C. Marchió); Instituto de Salud Carlos III grants PI051890 and RETICS:RD06/0020/0013 (J. Palacios); and Ramon y Cajal Programme 2004 junior research contract (G. Moreno-Bueno).

The costs of publication of this article were defrayed in part by the payment of page charges. This article must therefore be hereby marked *advertisement* in accordance with 18 U.S.C. Section 1734 solely to indicate this fact.

**Note:** Supplementary data for this article are available at Clinical Cancer Research Online (http://clincancerres.aacrjournals.org/).

**Requests for reprints:** Jorge S. Reis-Filho, The Breakthrough Breast Cancer Research Centre, Institute of Cancer Research, 237 Fulham Road, London SW3 6JB, United Kingdom. Phone: 44-207-153-5167; Fax: 44-207-512-5533; E-mail: jorge.reis-filho@icr.ac.uk.



doi:10.1158/1078-0432.CCR-08-1878

Tumor histologic grade remains one of the most powerful prognostic factors for breast cancer. In recent years, further prognostic information has been gleaned from expression profiling studies of invasive breast cancers where different breast cancer molecular subtypes (1) with distinct biological features and clinical outcome (2) have been identified. Nonetheless, even the "poor prognosis" molecular subtypes are significantly associated with high histologic grade. Hence, high-grade (grade 3) breast cancer as a whole continues to represent one of the most therapeutically challenging entities in clinical practice.

It is clear that despite the overall association with poor outcome, grade 3 breast cancers are composed of clinically, histologically, genetically, and transcriptomically distinct subgroups that encompass the molecular subtypes (basal-like, luminal, and HER-2 positive) described in the pioneering studies of Perou et al. (1, 2). Nielsen et al. (3) subsequently showed that a prognostically significant (3–5) surrogate panel of four immunohistochemical markers (estrogen receptor, epidermal growth factor receptor, HER-2, and cytokeratin 5/6) could be used to identify these molecular subgroups with a sensitivity of 76% and a specificity of 100% for the identification of

## Translational Relevance

Therapeutic approaches for the management of grade 3 invasive ductal carcinomas of no special type (IDC-NST) remain inadequate and additional therapeutic options are required. We analyzed 95 grade 3 IDC-NST, classified into the molecular subgroups (basal-like, HER-2, and luminal), using high-resolution microarray-based comparative genomic hybridization. Our analysis provided insights into the pattern of aberrations and type of genomic instability in each molecular subgroup of grade 3 IDC-NST and identified subgroup-specific recurrent amplifications harboring putative therapeutic targets. The amplicon 17q23.2 was found in 20% and 8% of HER-2 and luminal cancers, respectively. Using RNA interference, we show that expression of *PPM1D*, one of the genes pertaining to this amplicon, is required for the survival of cells harboring 17q23.2 amplification, suggesting that PPM1D may constitute a therapeutic target for subsets of HER-2 and luminal cancers. Our results show that this approach could facilitate the identification of new therapeutic targets for subgroups of breast cancer patients.

basal-like cancers. Recent comparative genomic hybridization (CGH) profiling studies have concentrated on defining genomic signatures for different breast cancer subgroups, with the aim of identifying common subtype-specific alterations (6–8). The results of these studies have suggested that basal-like tumors display complex genomic profiles and less frequently harbor amplifications (7), whereas luminal cancers more often show focal, high-level amplifications (7). These studies have also shown that deletions of the whole arm of 16q seem to be more frequently found in grade 1 luminal A breast cancers (9–12), whereas the majority of basal-like and HER-2 cancers (which are usually of high histologic grade) lack this genetic aberration. There is now increasing evidence suggesting that grade 3 and 1 breast cancers are clinically and genetically distinct entities and that progression from grade 1 to 3 breast cancer is an uncommon biological phenomenon (9, 10, 12). In fact, concurrent presence of grade 1 and 3 areas in the same specimen is seen in <10% of cases (13).

Current therapeutic approaches in the management of grade 3 breast cancer remain inadequate, particularly with regard to basal-like breast cancers that are usually of a high-grade triple-negative (estrogen receptor, progesterone receptor, and HER-2 negative) phenotype. Furthermore, even in the context of *HER-2*-amplified tumors, a significant proportion of patients either are *de novo* resistant or develop resistance to trastuzumab over time (14). Surprisingly, although the aforementioned studies have undoubtedly helped in cataloguing the molecular genetic and gene expression profiles of breast cancers, very few functionally validated therapeutic targets have emerged from them (8, 15). This may be related to low platform resolution (6, 7, 16), heterogeneity of samples analyzed with regard to grade and histologic type (6–8, 16), and the fact that many studies have used non-microdissected tissue (6–8).

Here, we have focused on the analysis of microdissected grade 3 invasive ductal carcinomas of no special type (IDC-NST). The aims of this study were 2-fold: (*a*) to characterize the molecular genetic profiles of grade 3 IDC-NST using a combination of high-resolution microarray-based CGH (aCGH) and *in situ* hybridization and (*b*) to identify recurrent amplicons harboring putative therapeutic targets associated with luminal, HER-2, and basal-like tumor phenotypes as defined by the criteria of Nielsen et al. (3). Unlike previous studies, we endeavored to define the molecular genetic features of grade 3 IDC-NST classified into the molecular subgroups (1–3) using a validated immunohistochemical surrogate (3), which is amenable to be applied for the classification of archival, formalin-fixed breast cancers.

## Materials and Methods

***Sample cohort.*** A series of grade 3 IDC-NST cases were retrieved from University Hospital La Paz and University of Munster. This project has been approved by the local research ethics committees of the authors' institutions. aCGH was done in 100 consecutive fresh/frozen samples of grade 3 IDC-NST from this combined series.

All cases were reviewed by three pathologists (S.M.R-P., H.B., and J.S.R-F.), and representative areas of 91 cases, where adequate representative paraffin blocks were available, were included in a tissue microarray (TMA-1) containing 1 mm replicate cores from each case. These cases were used to validate selected amplifications found in the aCGH analysis.

An independent cohort (TMA-2) was used in form of a second tissue microarray containing 120 grade 3 IDC-NST. These samples were obtained from consecutive patients who were diagnosed and treated at the Royal Marsden Hospital, with therapeutic surgery followed by anthracycline-based adjuvant chemotherapy. All patients with estrogen receptor-positive tumors also received adjuvant endocrine therapy. Details of both cohorts are provided in Supplementary Table S1.

***DNA extraction.*** Representative frozen sections (8 μm thick) of 104 grade 3 tumors were cut, mounted onto Superfrost glass slides, stained with nuclear fast red, and microdissected with a sterile needle under a stereomicroscope to obtain a percentage of tumor cells >75% as described previously (17). Genomic DNA was extracted as described previously (17). The concentration of the DNA was measured with Picogreen according to the manufacturer's instructions (Invitrogen).

***aCGH.*** The aCGH platform used for this study was constructed at the Breakthrough Breast Cancer Research Centre and comprises ~32,000 BAC clones tiled across the genome. Labeling, hybridization, washes, image acquisition, data normalization, and filtering were carried out as described previously (17). This type of BAC array platform has been shown to be as robust as and to have comparable resolution with high-density oligonucleotide arrays (18, 19). A final data set of 30,606 clones with unambiguous mapping information according to the March 2006 build (hg18) of the human genome[9] was used. Data were smoothed using a local polynomial adaptive weights smoothing (AWS) procedure for regression problems with additive errors (17). Thresholds for defining genomic gains and losses were obtained using data from unamplified female versus female and female versus male genomic DNA as described previously (17). Smoothed $\log_2$ ratio values less than -0.08 were categorized as losses, those >0.08 as gains, and those in between as unchanged. Amplifications were defined as smoothed $\log_2$ ratio values >0.4. Data processing and analysis was carried out in R 2.0.1[10] and BioConductor 1.5[11] using modified versions of the packages aCGH, marray, and AWS. Threshold data for each clone was also used for categorical analysis using a Fisher's exact

[9] http://www.ensembl.org
[10] http://www.r-project.org/
[11] http://www.bioconductor.org/

test adjusted for multiple testing using the step-down permutation procedure maxT, providing strong control of the family-wise type I error rate (17, 20). A false discovery rate-adjusted $P < 0.05$ was considered significant. Details of the 100 cases hybridized are described in Supplementary Table S1. Cluster analysis was done using the hclust function in R2.1.0 using AWS-smoothed ratios according to the Ward's method (20). Tumors were classified according to their pattern of genomic alterations, "simplex," "sawtooth," and "firestorm," as described (21).

***Immunohistochemistry.*** Sections (4 μm thick) of the tumors were subjected to a panel of immunohistochemical markers. Antibodies, antigen retrieval methods, and cutoffs are described in Supplementary Table S2. All markers were scored by at least two observers blinded to the results of the aCGH analysis. Tumors were classified into HER-2, luminal, and basal-like subgroups using the criteria of Nielsen et al. (3).

***Fluorescence and chromogenic* in situ *hybridization.*** Chromogenic *in situ* hybridization (CISH) for *HER-2*, *CCND1*, and *EGFR* was done using the ready-to-use digoxigenin-labeled SpotLight gene amplification probes (Invitrogen) and fluorescence *in situ* hybridization analysis with BAC RP11-372I05 (*CCNE1*) was done using in-house, biotin-labeled probes as described previously (22). Pretreatment, digestion, and hybridizations were done as described by Lambros et al. (22). For CISH and fluorescence *in situ* hybridization analysis, at least 60 nonoverlapping nuclei of morphologically unequivocal neoplastic cells were analyzed. Cases were considered amplified by CISH if >50% of neoplastic cells harbored large signal clusters or >5 signals/nucleus. CISH and fluorescence *in situ* hybridization analysis were carried out with observers blinded to the results of aCGH analysis.

***Quantitative real-time PCR.*** Representative frozen sections (8 μm thick) of 55 of 95 grade 3 tumors classified as basal-like, luminal, or HER-2 and subjected to aCGH analysis (no material was available for 40 cases) were microdissected as described above to obtain a percentage of tumor cells >75% (17). RNA was extracted using Trizol according to the manufacturer's instructions (Invitrogen) and quantified using the Agilent 2100 Bioanalyzer with RNA Nano LabChip kits (Agilent Biosystems). First-strand synthesis was done as described previously (23) and quantitative real-time PCR was done using TaqMan chemistry on the ABI Prism 7900HT (Applied Biosystems) using the standard curve method. Assays were purchased from Applied Biosystems, except for TBP, which was designed as described previously (23). Each gene of interest was normalized to the geometric mean of the three references (TBP, TFRC, and MRPL19; Assay-on-Demand ID: Hs00174609_m1-TFRC, Hs00608522_g1-MRPL19, and Hs00186230_m1-PPM1D).

***Statistical analysis.*** Statistical analysis of tissue microarray data (immunohistochemistry and CISH) was done with SPSS package (version 11.5). Fisher's exact and $\chi^2$ tests were done with a two-tailed $P$ value; 95% confidence intervals were employed for all tests.

***Cell lines.*** Cell lines representative of the HER-2 subtype (BT474, MDA-MB-361, and ZR-75.30), luminal subtype (MCF-7, CAMA1, T47D, KPL-1, MCF-3B, and ZR-75.1), basal-like subtype (MDA-MB-231) and HeLa were obtained from the American Type Culture Collection and maintained as described previously (16).

***Plasmids.*** Cells were transfected with a previously validated pSUPER plasmid known to silence PPM1D expression (24) and an additional plasmid expressing the blasticidin resistance gene (pEFBsd; Invitrogen) in a molar ratio of 10:1. Transfections were carried out using Lipofectamine 2000 (Invitrogen) or FuGene (Roche) according to the manufacturers' instructions. Silencing of PPM1D following stable transfection with pSUPER-PPM1D short hairpin RNA has been shown previously (24).

***Sulforhodamine B colorimetric assay for cytotoxicity.*** Sulforhodamine B colorimetric assay for cytotoxicity (25) using short hairpin RNA-mediated PPM1D knockdown and a small-molecule PPM1D inhibitor (CCT007093) were done as described previously (24). Briefly, cells were transfected with a pSUPER plasmid and an additional plasmid expressing the blasticidin resistance gene (pEFBsd; Invitrogen) in a molar ratio of 10:1. Cells were plated in 6-well plates 24 h after transfection. Blasticidin selection (5 μg/mL) was initiated 48 h post-transfection and replenished every 3 days. For chemical inhibition of PPM1D, cells were plated in 6-well plates and treated with CCT007093. Medium and inhibitor were replenished every 3 days. Cells were fixed in 3.3% TCA after 14 days and viable cells were quantified using the sulforhodamine B assay as described previously (25). Experiments were done in triplicate.

***Antibodies.*** Total protein lysates (100 μg) were separated by SDS-PAGE according to standard protocols, and immunoblotting was carried out using primary antibodies directed against PPM1D as described previously (24), anti-TP53 (Neomarkers), anti-p38 rabbit polyclonal antibody (Cell Signaling), anti-ERBB2/Neu (Santa Cruz Biotechnology), and anti-β-tubulin (Sigma). Western blots were scanned and quantitated using PDQuest and Quantity One software (Bio-Rad). Background was subtracted and the intensity of PPM1D was compared relative with that of β-tubulin.

## Results

***Breast cancer molecular classification.*** Using the immunohistochemical panel described by Nielsen et al. (3), of the 104 microdissected grade 3 IDC-NST, 45 were of luminal, 25 of basal-like, 25 of HER-2, and 9 of indeterminate phenotype. Details of the aCGH and tissue microarray cohorts, used to validate the results of the aCGH findings, are summarized in Table 1, Supplementary Table S1, and Supplementary Fig. S1. The 95 cases classified into the molecular subgroups were subjected to aCGH. Of the 9 cases of indeterminate phenotype, sufficient DNA was obtained from 5 cases (Supplementary Fig. S2). Given the heterogeneity of tumors of indeterminate phenotype and the small sample size, these samples were not included in subsequent analysis. Full details of both tissue microarray cohorts are described in Supplementary Table S1.

***Genetic profiling of grade 3 tumors.*** In the cohort of 95 grade 3 IDC-NST, the most prevalent recurrent genetic aberrations included gains of 1q (60%) and 8q (75%) and losses of 1p (60%), 8p (60%), and 17p (60%; Fig. 1A). The most prevalent amplifications affected 1q, 8q, and 17q. The pattern and prevalence of genetic aberrations in these cases when classified according to the criteria of Nielsen et al. (3) are shown in Fig. 1B and C. Selected genomic aberrations were validated by fluorescence *in situ* hybridization/CISH. In brief, amplifications of *HER-2*, *CCND1*, and *EGFR* were validated in all but one case (Supplementary Fig. S1). Noteworthy, amplification of *ESR1* was found in only 1 of 95 cases, in line with recently reported results (26–28).

***Basal-like, luminal, and HER-2 tumors have distinct genetic patterns.*** Using the criteria recently defined by Hicks et al. (21), 15 of 95 (16%) had a "simplex" pattern characterized by low-level whole-arm gains and losses, 40 of 95 (42%) of cases had a complex "sawtooth" pattern, with multiple gains and losses across the entire genome, and 40 of 95 (42%) had a "firestorm" pattern of genomic alterations defined by resembling the "simplex" type with at least one localized region of clustered, relatively narrow peaks of amplification, with each cluster confined to a single chromosome arm. A statistically significant correlation between molecular subtype and pattern of genetic aberrations was observed (Table 2): 72% of basal-like cancers displayed a "sawtooth" pattern, whereas 88% of HER-2 tumors harbored a "firestorm" pattern. As expected, given the high histologic grade, the majority of luminal cancers displayed either "sawtooth" (42%) or firestorm (33%) patterns.

**Table 1.** Clinicopathologic characteristics of 69 grade 3 tumors used for aCGH analysis with clinical data available used for aCGH from the University Hospital La Paz series

| | Basal-like | Luminal | HER-2 |
|---|---|---|---|
| Samples (*n*) | 14 | 37 | 18 |
| Age, median (range) | 52.5 (30-70) | 55 (31-81) | 49.5 (30-80) |
| Lymph node status (% positive) | 42.9 | 65.7 | 44.4 |
| Stage (pT) | | | |
| 1 | 28.6 | 45.9 | 44.4 |
| 2 | 71.4 | 45.9 | 44.4 |
| 3 | 0 | 5.4 | 5.6 |
| 4 | 0 | 2.8 | 5.6 |
| Size (mm), median (range) | 23.5 (17.0-38.0) | 22.0 (12.0-8.00) | 22.5 (15.0-70.0) |

NOTE: Clinicopathologic characteristics of grade 3 IDC-NST subjected to aCGH analysis. Note that in 26 cancers no clinical data were available due to anonymization.

Interestingly, 25% of luminal cancers displayed a "simplex" pattern, characterized by gains of 1q and deletions of 16q, which are often found in luminal A cancers (6, 7).

Unsupervised hierarchical clustering using AWS-smoothed data provided additional support for the associations between basal-like cancers and "sawtooth" genetic profiles and HER-2 phenotype and "firestorm" genetic patterns (Fig. 2A). One cluster was entirely composed of tumors with a "sawtooth" pattern and significantly enriched for basal-like cancers ($P < 0.0001$, Fisher's exact test). A second cluster composed of tumors predominantly of "firestorm" pattern was significantly enriched for HER-2 cancers ($P < 0.0001$, Fisher's exact test). The remaining three clusters were predominately populated by tumors of luminal phenotype (Fig. 2A). It should be noted that given the lack of publicly available microdissected breast cancers subjected to tiling path aCGH analysis to cross validate our findings, this heat map should be perceived as hypothesis-generating and not as a class discovery exercise.

***Progression from grade 1 to 3 IDC-NST cannot be ruled out in tumors of luminal phenotype.*** Loss of the whole arm of chromosome 16q has been shown to be found in >85% of grade 1 IDC-NST and <20% of their grade 3 counterparts (9–11). These data have been interpreted as evidence to suggest that grade 3 cancers are not the results of progression of grade 1 breast cancers (9–12, 29, 30). However, more recent studies have suggested that this model could be more complex and that there could be a group of grade 3 breast cancers progressing through grades, with subsequent accumulation of gains, losses, and amplifications in the higher-grade lesions (13, 29, 30). In the present study, loss of the entire chromosome 16q, as described in low-grade breast cancers, was observed in 30% of all our grade 3 cancers (Fig. 1A). Interestingly, loss of the whole arm was more frequently found in grade 3 IDC-NST luminal cancers than in nonluminal cancers (44% versus 22%; $P = 0.0049$, Fisher's exact test, Fig. 2B). Taken together, our results suggest that progression from low-grade to high-grade IDC-NST cannot be ruled out in 44% of tumors of luminal phenotype, whereas, in basal-like and *HER-2*-amplified cancers, 16q deletions are significantly less frequent, suggesting that the possibility of progression from low-grade to high-grade breast cancers in these groups is less likely.

***Genomic profiles of basal-like tumors.*** The most prevalent alterations (>50%) found in basal-like tumors were whole-arm gains of 1q, 6p, 8q, and 10p and losses of 1p, 4p, 5q, 8p, 10q, 15q, and Xp (Fig. 1B; Supplementary Table S3). Recurrent high-level gains/amplifications were found on 1q21, 3q25, 8q24, 12p13, and 19q12 (Fig. 1B and C; Supplementary Table S4). Using a multi-Fisher's exact test with *P* values adjusted for multiple comparisons (17, 20), we were able to identify the differences in the genetic profiles between basal-like and non-basal-like (luminal and HER-2) tumors.

Chromosomal regions differentially associated with basal-like phenotype are illustrated in Fig. 2C and summarized in Table 3 and Supplementary Tables S3 to S7. When compared with non-basal-like tumors, basal-like cancers were characterized by losses of 2q27.3, 4p16.1, 5q, 7p15, 10q25, 12q, 15q13, and 16p and gains of 1p12, 2p22, 6p22-p21, 7q11-q23, 9p24-p13, 10p15-p11, 10q11, and 12p13 and high-level gains/amplifications of 1q21.1, 3q25.1-q25.2, 8q24.21-8q24.23, 9p24.2-p22.3, 10p15.3-p15.2, 12p13.33-12p13.31, 12p13.2, 12p13.11, 12p12.1, 12p11.23-p11.22, 12p11.21, 19q12, and 19q13.2.

By comparing each tumor subgroup in a pair-wise fashion, we found that losses of 15q14-q21 and gains of 10p15 were preferentially found in basal-like breast cancers when compared with HER-2 tumors. Compared with luminal cancers, basal-like breast cancers more frequently harbored losses of 4p16-p15, 5q, 7p15-p12, 10q25, 12q23-q24, and 16p13-p12 and gains of 6p24-q21, 7q31-q33, 9p25-p21, 10p15-p21, 10q11-q21, and 12p13 and high-level gains/amplifications of 1q21.1, 8q24.21-q24.23, 10p14, 12p13.31, 12p12.1, 12p11.23-p11.22, and 19q12. Comparing our data with those of recently reported whole-genome aCGH studies (7, 8), novel high-level gains/amplifications associated with basal-like phenotype were found on 3q25.1, 9p24, and 19q13. Moreover, 12p13 amplification, reported previously to be specifically associated with basal-like breast cancer of medullary type (31), is also found in grade 3 IDC-NST of basal-like phenotype.

***Genomic profiles of luminal tumors.*** The most prevalent alterations (>50%) found in luminal tumors were whole-arm gains of 1q, 8q, and 20q and losses of 1p, 8p, 11q, 16q, and 17p. Recurrent high-level gains/amplifications were found on 1q31.3-q32.3, 8p11.21, 8q21-q24, 11q13-q14, and 17q21-q25 (Fig. 1B and C; Supplementary Table S8).

Compared with nonluminal tumors, luminal cancers were characterized by gains of 5q, 11q13, 16p12, and 20q and

amplifications of 1q32.1, 1q32.2, 8p12, 11q13.2, and 11q13.4-q14.1 (Fig. 2B). Compared with basal-like breast cancers, luminal tumors preferentially harbored gains of 5q11.2-q12.1, 8q24.23-q24.3, 12q21.2, and 20q11.23, losses of 6q22.33-q24.1, 11q23.1-q23.3, and 11q24.1-q24.2, and amplification of 11q13.2-q13.3. Compared with HER-2 tumors, luminal cancers were characterized by high-level gains/amplification of 8p12.

***Genomic profiles of HER-2 tumors.*** HER-2 tumors were characterized by a high frequency (>50%) of gains of 1q, 8q, and 17q and losses of 1p, 8p, and 17p and focal loss of 17q22. Recurrent high-level gains/amplifications were identified on

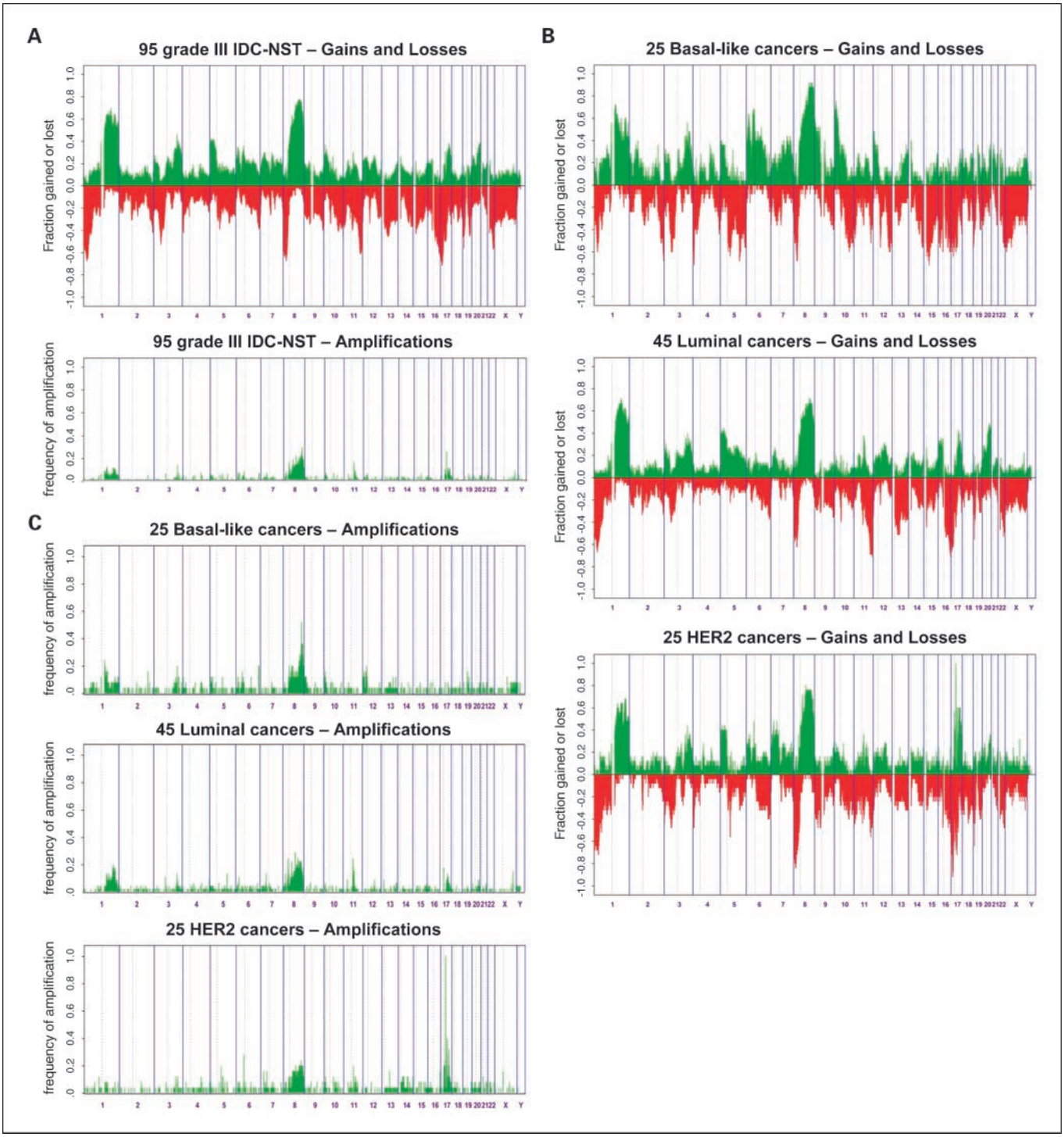


**Fig. 1.** Genomic alterations in 95 grade 3 IDC-NST breast cancers. The proportion of tumors in which each clone is altered (*green columns,* gains or amplifications; *red columns,* losses) is plotted (*Y axis*) for each BAC clone according to genomic location (*X axis*). *Vertical dotted lines,* chromosome centromeres. *A,* 95 grade 3 IDC-NST (gains, losses, and amplifications). *B,* frequency of gains and losses according to the molecular subgroups: basal-like, luminal, and HER-2. *C,* frequency of amplifications according to the molecular subgroups: basal-like, luminal, and HER-2.

**Table 2.** Correlation between genomic pattern (21) and molecular phenotype (3) of 95 grade 3 IDC-NST

| Genomic pattern | Luminal (%) | Basal (%) | Her2 (%) |
|---|---|---|---|
| Simplex | 25 | 16 | 0 |
| Complex sawtooth | 42 | 72 | 12 |
| Complex firestorm | 33 | 12 | 88 |

$P = 0.0001$ (Fisher's $3 \times 3$ test)

7p15, 7p14, 8q21-q24, 11q13.2-q13.3, 14q11.1-q11.2, 14q12-q13.1, and 14q23.2-q23.3 and multiple loci on 17q, 19q13.41, 21q22.3, and 22q11 (Fig. 1B and C; Supplementary Table S9). All cases classified as HER-2 cancers were shown to harbor *HER-2* gene amplification at 17q12 by aCGH, which was confirmed by CISH (Supplementary Table S1).

Compared with non-HER-2 tumors, HER-2 cancers were found to harbor gains of 17q11.2, 17q12-q21.2, and 17q21.32-q21.33, losses of 17q22, and amplifications of 14q12-q13.1, 14q23.1-q23.3, 17q12, 17q21.32-q22, 17q23.1-q23.2, and 17q23.2 (Fig. 2D). Compared with basal-like tumors, HER-2 cancers had differential gains of 17q, loss of 9p21.3, and amplification of 17q12-q21.2 and 17q23.2. HER-2 tumors more frequently displayed gains of 17q11-q12 and 17q21, loss of 17q22, and amplifications of 17q12-q21.2, 17q21.32-q21.33, and 17q23.2 when directly compared with luminal tumors. Novel amplifications associated with HER-2 phenotype were found on 14q12-q13.1, 14q23.2-q23.3, 17q21.32-q22, and 17q23.1-q23.2 (Supplementary Table S6 and S7).

***17q23.2 is frequently amplified in HER-2 and luminal cancers.*** By performing a Fisher's test between the phenotypic groups as defined by the criteria of Nielsen et al. (3), we identified amplification of 17q23.2 as significantly associated with tumors of HER-2 and luminal phenotype (inversely associated with basal-like phenotype). This amplification maps to 55.503 to 57.374 kb and was found in 8% (8 of 95) of grade 3 IDC-NST: 7% of luminal, 20% of HER-2, and 0% of basal-like cancers ($P = 0.033$, $\chi^2$ test; Fig. 3A). This region encompasses several known genes: *TBX2*, *TBX4*, *CA4*, *C17orf64*, *APPBP2*, *INTS2*, *LOC388407*, *USP32*, *BRIP1*, *PPM1D*, *NACA2*, and *BCAS3*. Analysis of publicly available data retrieved from Neve et al. (16) and Adelaide et al. (8) showed that of all genes mapping to the smallest region of amplification for which expression data were available, the only genes whose expression was significantly correlated with gene amplification were *PPM1D*, *BCAS3*, *USP32*, and *BRIP1*. No correlations between 17q23.2 amplification gene amplification and p53 immunohistochemical expression were found ($P > 0.1$, Fisher's exact test; Supplementary Table S1).

Previous studies have suggested that the likeliest oncogenes driving this amplicon would be *RPS6KB1*, *TBX2*, and *PPM1D* (32). Here, we show that *RPS6KB1* does not map to the smallest region of overlap of 17q23.2 amplicon. Furthermore, *TBX2* expression levels failed to correlate with gene amplification in two independent data sets (7, 8, 16). On the other hand, PPM1D has been shown to have oncogenic properties (32–34), has expression levels that correlate with gene copy number, and localizes to the smallest region of amplification.

Quantitative real-time PCR done with RNA extracted from microdissected primary tumor samples from our series (Fig. 3B) revealed a significant correlation between high levels of *PPM1D* expression and amplification at 17q23.2 ($P = 0.0002$, Mann-Whitney *U* test). PPM1D expression was significantly lower in basal-like cancers when compared with luminal and HER-2 cancers ($P = 0.0175$, two-tailed unpaired *t* test, heteroscedastic; Supplementary Table S1). No correlations between PPM1D mRNA expression and p53 immunohistochemical expression were found in primary breast cancers ($P > 0.1$, two-tailed unpaired *t* test, heteroscedastic; Supplementary Table S1).

***PPM1D is one of the amplicon drivers of 17q23.2 and a putative therapeutic target for a subgroup of luminal and HER-2 cancers.*** Given that 17q23.2 was one of the most commonly amplified regions in HER-2-positive cancers (20%) and also found in luminal tumors (8%) and the fact that PPM1D has been shown to have oncogenic properties (33, 34) and to be a protein amenable to targeting with small-molecule inhibitors (24), we investigated whether PPM1D would be one of the drivers of the 17q23.2 amplicon. *PPM1D* encodes a serine/threonine phosphatase and has been described previously as an oncogene and potential therapeutic target (24). Given the expression of PPM1D in primary breast cancers harboring the 17q23.2 amplification (Fig. 3B), we tested whether *PPM1D* would be consistently overexpressed when amplified in 11 breast cancer cell lines (Figs. 3C and D and 4A). Quantitative real-time PCR analysis of these cell lines showed a strong correlation between *PPM1D* gene amplification and PPM1D mRNA levels ($P = 0.002$, Mann-Whitney *U* test; Fig. 4A). In fact, the lowest levels of *PPM1D* expression in *PPM1D*-amplified cell lines (from BT474 cells) were two times higher than the highest levels of *PPM1D* mRNA in cells not harboring this amplification (ZR-75.1; Fig. 4A). In addition, cell lines harboring *PPM1D* amplification expressed significantly higher levels of PPM1D protein as defined by densitometric analysis of Western blots ($P < 0.004$, Mann-Whitney *U* test; Fig. 4B; Supplementary Fig. S3).

We next interrogated whether PPM1D expression is required for tumor cell viability in cells harboring amplification of this gene. Cell lines were initially assessed for expression of PPM1D, HER-2, p53, and p38 proteins by Western blotting (Fig. 4B). Then, we silenced PPM1D in *in vitro* models of HER-2 (BT474 and ZR-75.30) and luminal (MCF-7, KPL-1, and MCF-3B) tumors harboring the 17q23.2 amplification (35) by transfection of a previously validated short hairpin RNA-expressing plasmid (24). PPM1D silencing resulted in significantly greater loss of viability in *PPM1D*-amplified and overexpressing cells (BT474, MCF-7, KPL-1, MCF-3B, and ZR-75.30) when compared with cells harboring normal copy numbers of *PPM1D* (MDA-MB-231, MDA-MB-361, T47D, CAMA1, ZR-75.1, and HeLa; Fig. 4C). We next tested whether PPM1D phosphatase activity would be required for the survival of cells harboring *PPM1D* amplification by treating these cells and nonamplified cell lines with the PPM1D inhibitor CCT007093 (Fig. 4D; ref. 24). *PPM1D*-amplified cell lines (BT474, MCF-7, KPL-1, MCF-3B, and ZR-75.30) displayed a significantly increased sensitivity to CCT007093 compared with cells harboring normal copy numbers of *PPM1D* (MDA-MB-231, MDA-MB-361, T47D, CAMA1,

ZR-75.1, and HeLa). These results provide strong circumstantial evidence to suggest that *PPM1D* is one of the drivers of the 17q23.2 amplicon and may constitute a therapeutic target for breast cancers of luminal and HER-2 phenotype harboring this amplification.

## Discussion

Here, we employed tiling path BAC arrays to characterize the genetic profiles of grade 3 IDC-NST. Although more recent technologies, such as oligonucleotide arrays and molecular

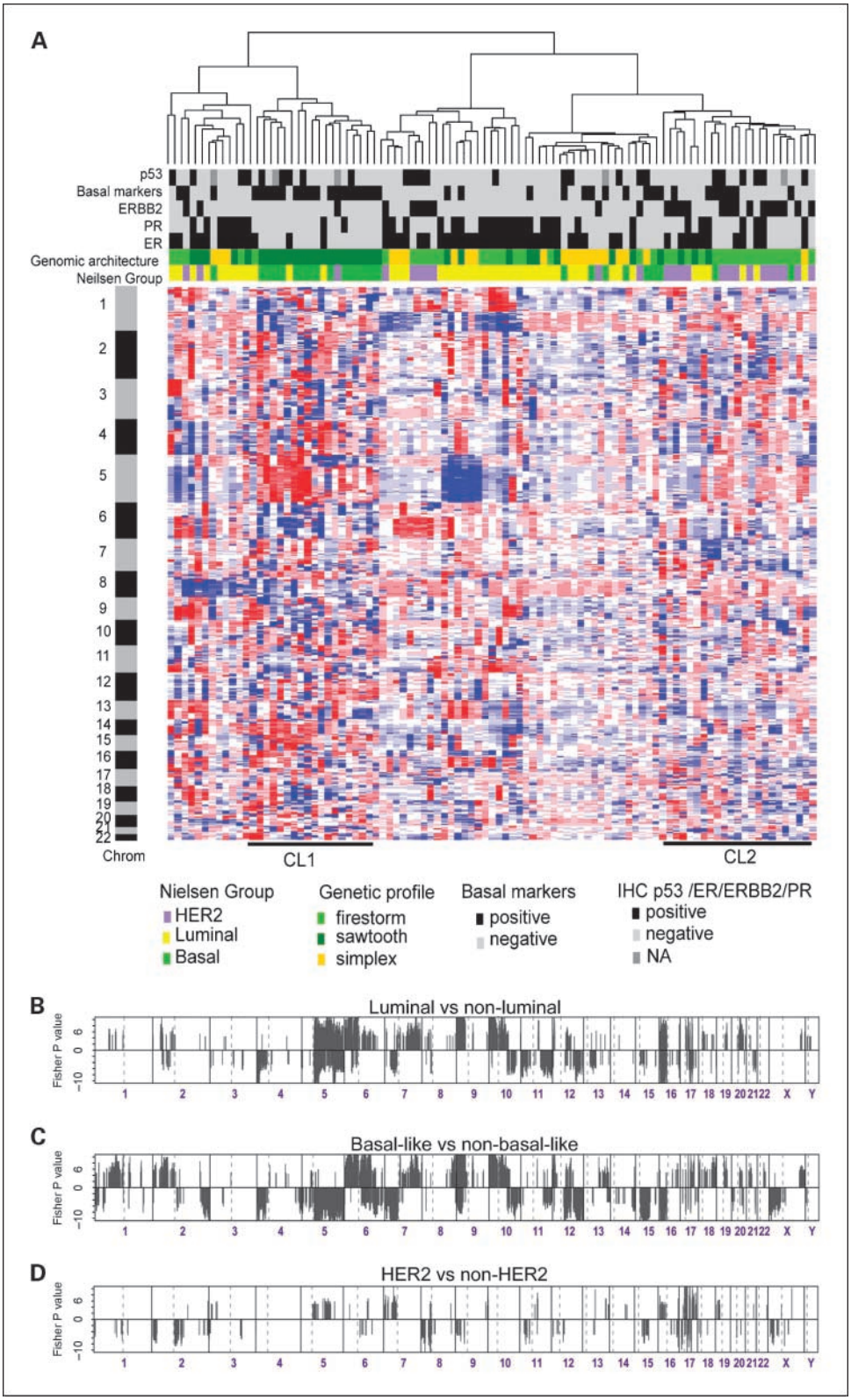


**Fig. 2.** Unsupervised and supervised analysis of copy number aberrations in relation to breast cancer molecular subgroups. *A,* heat map of aCGH data for grade 3 IDC-NST. *Rows,* AWS-smoothed data as gains (*blue*), losses (*red*), or no change (*white*) for each BAC clone in genome order. Note the presence of a cluster significantly enriched for tumors of basal-like phenotype and "sawtooth" genetic profiles (CL1) and another significantly enriched for tumors of HER-2 phenotype and "firestorm" genetic profile (CL2). *B,* multi-Fisher's comparison between luminal and nonluminal grade 3 IDC-NST. *C,* multi-Fisher's comparison between basal-like and non-basal-like grade 3 IDC-NST. *D,* multi-Fisher's comparison between HER-2 and non-HER-2 grade 3 IDC-NST. *B* to *D*, multi-Fisher's exact tests are carried out on the segmented values for each clone, and those with a permutation corrected $P < 0.05$ are plotted (inverse log *P* value; *Y axis*) according to genomic location (*X axis*). *Bottom,* clones with a significant nonadjusted $P < 0.05$ (*Y axis*) before correction for multiple testing plotted according to the genomic position (*X axis*). *Negative values, P* values associated with loss of a region. For adjusted *P* values, see Supplementary Table S3.

**Table 3.** Regions of amplification associated with tumor phenotype

**Basal**

| Chromosome | Start (Mb) | End (Mb) | Cytoband | Basal (%) | Non-basal (%) | Adjusted Fisher's *P* |
|---|---|---|---|---|---|---|
| 1 | 142.8 | 143.33 | q21.1 | 20 | 3 | 0.02 |
| 1 | 143.9 | 144.96 | q21.1 | 20 | 1 | 0.01 |
| 1 | 146.33 | 147.04 | q21.1 | 20 | 3 | 0.02 |
| 3 | 152.71 | 154.22 | q25.1-q25.2 | 12 | 0 | 0.03 |
| 3 | 170.14 | 170.84 | q26.2 | 12 | 0 | 0.03 |
| 3 | 170.66 | 170.31 | q26.2 | 12 | 0 | 0.03 |
| 6 | 44.01 | 44.17 | p21.1 | 16 | 14 | 0.03 |
| 6 | 44.12 | 44.22 | p21.1 | 12 | 0 | 0.03 |
| 8 | 128.34 | 128.89 | q24.21 | 50 | 21 | 0.02 |
| 8 | 131.21 | 137.02 | q24.21-q24.23 | 36 | 11 | 0.02 |
| 9 | 4.12 | 5.34 | p24.2-p24.1 | 12 | 0 | 0.03 |
| 9 | 6.84 | 15.06 | p24.1-p22.3 | 12 | 0 | 0.03 |
| 10 | 0.17 | 0.91 | p15.3 | 12 | 0 | 0.03 |
| 10 | 1.47 | 3.34 | p15.3-p15.2 | 12 | 0 | 0.03 |
| 11 | 68.77 | 69.3 | q13.2-q13.3 | 0 | 20 | 0.02 |
| 11 | 69.34 | 70.01 | q13.3 | 0 | 20 | 0.03 |
| 12 | 1.72 | 2.52 | p13.33 | 12 | 0 | 0.03 |
| 12 | 2.98 | 3.79 | p13.33-p13.32 | 12 | 0 | 0.01 |
| 12 | 4.47 | 6.1 | p13.32-p13.31 | 12 | 0 | 0.03 |
| 12 | 9.14 | 9.28 | p13.31 | 16 | 0 | 0.01 |
| 12 | 11.69 | 12.26 | p13.2 | 12 | 0 | 0.03 |
| 12 | 13.45 | 13.75 | p13.1 | 12 | 0 | 0.03 |
| 12 | 21.89 | 25.69 | p12.1 | 16 | 1 | <0.0272 |
| 12 | 26.33 | 28.29 | p11.23-p11.22 | 16 | 1 | <0.0277 |
| 12 | 30.97 | 31.38 | p11.21 | 12 | 0 | 0.03 |
| 17 | 34.78 | 35.52 | q12-q21.1 | 0 | 36 | <0.0157 |
| 19 | 33.86 | 34.13 | q12 | 12 | 0 | 0.03 |
| 19 | 34.64 | 34.91 | q12 | 16 | 1 | 0.03 |
| 19 | 45.12 | 45.53 | q13.2 | 12 | 0 | 0.03 |

**Luminal**

| Chromosome | Start (Mb) | End (Mb) | Cytoband | Luminal (%) | Nonluminal (%) | Adjusted Fisher's *P* |
|---|---|---|---|---|---|---|
| 1 | 199.22 | 199.76 | q32.1 | 11 | 0 | 0.04 |
| 1 | 200.7 | 201.43 | q32.1 | 11 | 0 | 0.04 |
| 1 | 202.28 | 203.58 | q32.1 | 15 | 0 | <0.0355 |
| 1 | 207.55 | 208.1 | q32.2 | 20 | 4 | 0.04 |
| 8 | 37.56 | 37.71 | p12 | 24 | 6 | 0.03 |
| 8 | 37.92 | 38.19 | p12 | 16 | 2 | 0.04 |
| 10 | 8.12 | 8.86 | p14 | 16 | 4 | 0.05 |
| 11 | 69.69 | 69.9 | q13.3 | 22 | 4 | 0.02 |
| 11 | 69.98 | 70.2 | q13.4 | 18 | 2 | 0.02 |
| 11 | 74.18 | 77.29 | q13.4-q14.1 | 15 | 0 | <0.0418 |
| 12 | 27.93 | 28.2 | p11.22 | 20 | 2 | 0.05 |
| 17 | 45.02 | 46.38 | q21.33 | 28 | 0 | <0.0465 |

**HER-2**

| Chromosome | Start (Mb) | End (Mb) | Cytoband | HER-2 (%) | Non-HER-2 (%) | Adjusted Fisher's *P* |
|---|---|---|---|---|---|---|
| 14 | 29.03 | 30.48 | q12 | 12 | 0 | 0.03 |
| 14 | 31.2 | 32.09 | q12-q13.1 | 12 | 0 | 0.03 |
| 14 | 64 | 64.42 | q23.2-q23.3 | 12 | 0 | 0.03 |
| 17 | 35.5 | 35.89 | q21.1-q21.2 | 100 | 0 | <0.0001 |
| 17 | 42.83 | 43.79 | q21.32 | 13 | 0 | <0.0272 |
| 17 | 44 | 47.68 | q21.32-q22 | 20 | 3 | <0.0272 |
| 17 | 55.5 | 57.37 | q23.1-q23.2 | 20 | 4 | <0.0464 |
| 17 | 59.2 | 59.5 | q23.3 | 20 | 4 | 0.05 |

NOTE: Regions of amplification associated with molecular subtype in a series of 95 grade 3 IDC-NST. Summary of the regions of chromosomal high-level gains/amplifications significantly associated with basal-like, luminal, and HER-2 tumors. Genes mapping to these regions are summarized in Supplementary Table S6. Percentages are frequency of alterations.

inversion probe arrays, are better suited for the identification of small alterations (e.g., microdeletions) and have a higher theoretical resolution, tiling path BAC arrays represent a robust and sensitive platform for the detection of recurrent gains, losses, and amplifications (refs. 18, 19 and references therein). Using this method, we show that the molecular phenotype of grade 3 IDC-NST correlates with the genomic pattern and the type of genetic aberration. In fact, HER-2 cancers more frequently harbored a "firestorm"/amplifier pattern and basal-like cancers more often showed a complex "sawtooth" pattern. It is possible that these differences reflect the type of genomic instability or the type of DNA repair dysfunction associated with each phenotypic group and also the distinct mechanisms of evolution and progression of these tumors. In fact, the molecular genetic characteristics of basal-like cancers identified in this study are remarkably similar to those described for tumors arising in *BRCA1* mutation carriers, gains of 3q, 10p, and 12p and losses of 4q, 5p, and 5q (36). Interestingly, we (37) and others (38) have recently shown that sporadic basal-like cancers and BRCA1 cancers have striking similarities in terms of their morphologic, immunohistochemical, and transcriptomic features and that sporadic basal-like cancers may have a dysfunctional BRCA1 pathway (37). Taken together, these data suggest that the type of genomic instability found

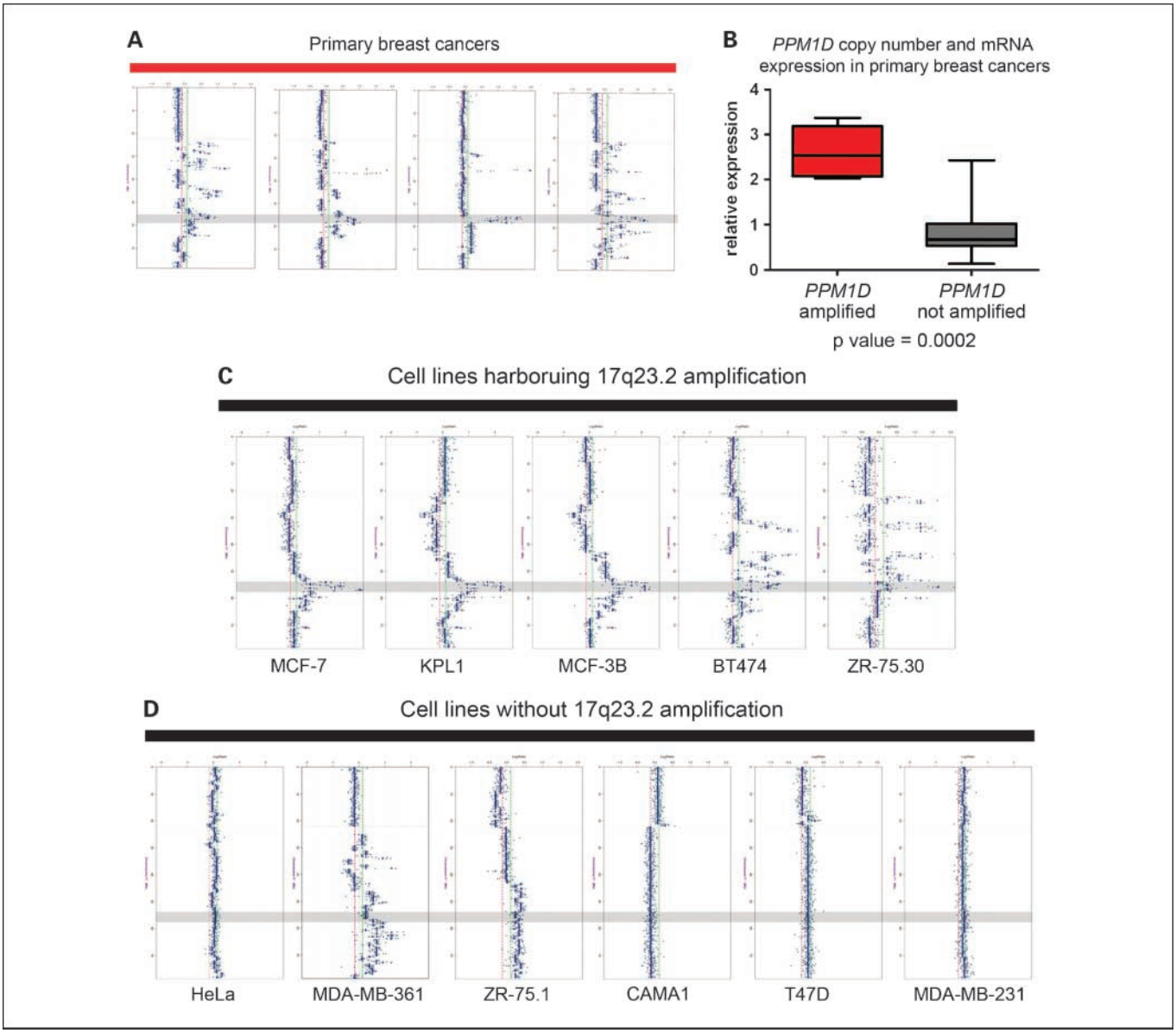


**Fig. 3.** 17q23.2 amplification in primary breast cancers and breast cancer cell lines. *A,* representative chromosome 17 plots of primary grade 3 IDC-NST with 17q23.2 amplification. $\log_2$ ratios are plotted (*X axis*) against each clone according to genomic location (*Y axis*). *Horizontal dotted line,* centromere. AWS-smoothed ratios are co-plotted (*blue*). *Gray box,* common region of amplification at 17q23.2. *B,* quantitative real-time PCR of PPM1D in 55 microdissected primary tumor samples, showing significant association of *PPM1D* mRNA overexpression and gene amplification. *C,* representative chromosome 17 plots of breast cancer cell lines harboring 17q23.2 amplification. $\log_2$ ratios are plotted (*X axis*) against each clone according to genomic location (*Y axis*). *Horizontal dotted line,* centromere. AWS-smoothed ratios are co-plotted (*blue*). *Gray box,* common region of amplification at 17q23.2. *D,* representative chromosome 17 plots of breast cancer cell lines lacking 17q23.2 amplification. $\log_2$ ratios are plotted (*X axis*) against each clone according to genomic location (*Y axis*). *Horizontal dotted line,* centromere. AWS-smoothed ratios are co-plotted (*blue*). *Gray box,* absence of 17q23.2 amplification.

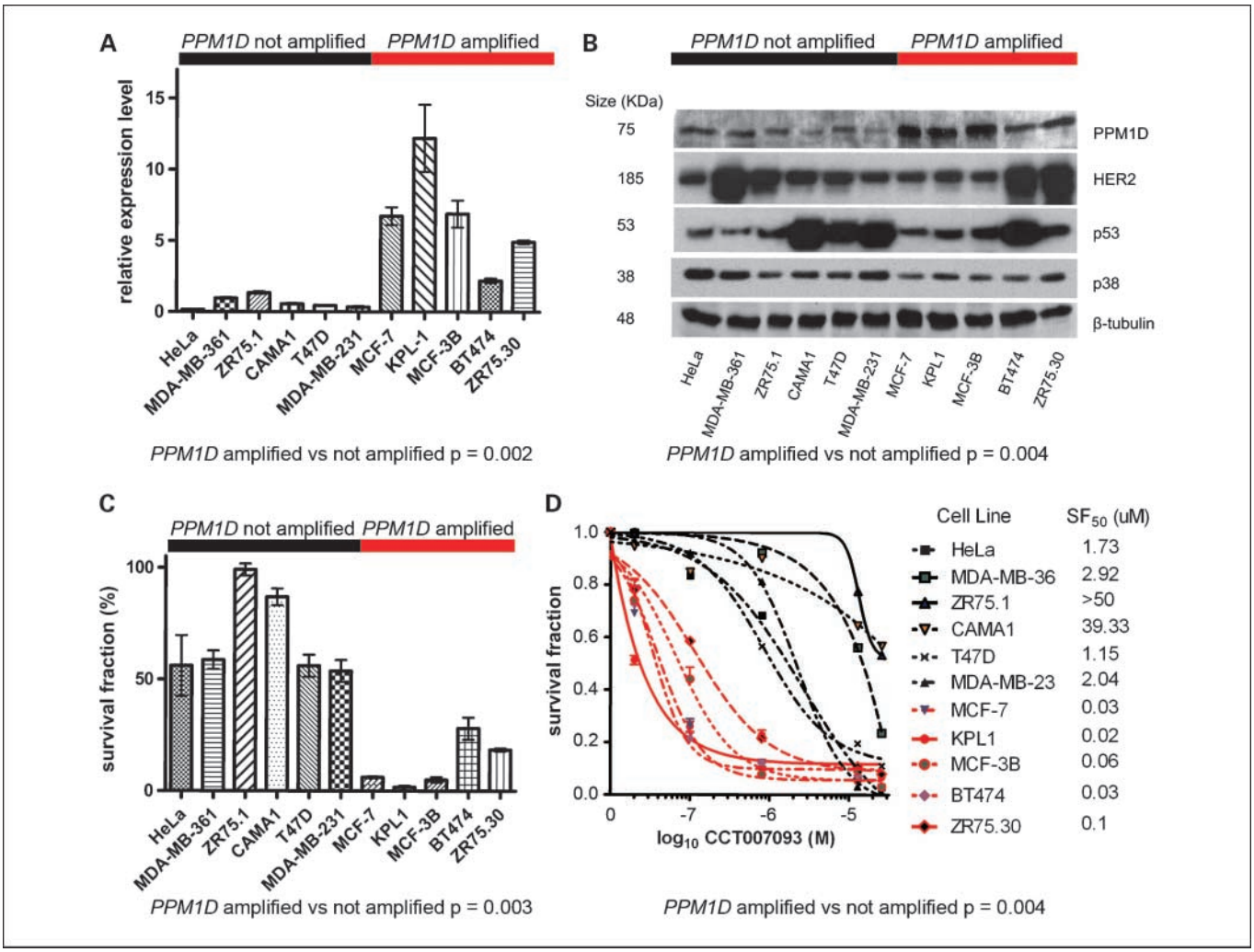


**Fig. 4.** PPM1D expression is required for the survival of breast cancer cells harboring 17q23.2 amplification and PPM1D overexpression. *A,* quantitative real-time PCR of *PPM1D* in 11 breast cancer cell lines showing a significant association between *PPM1D* mRNA overexpression and gene amplification. *B,* PPM1D, HER-2, p53, p38, and β-tubulin (loading control) expression of breast cancer cell lines by Western blot analysis. HeLa (control, *PPM1D* not amplified), MDA-MB-361 (*HER-2* amplified, *PPM1D* not amplified), ZR-75.1 (luminal, *PPM1D* not amplified), CAMA1 (luminal, *PPM1D* not amplified), T47D (luminal, *PPM1D* not amplified), MDA-MB-231 (basal-like, *PPM1D* not amplified), MCF-7 (luminal, *PPM1D* amplified), KPL-1 (luminal, *PPM1D* amplified), MCF-3B (luminal, *PPM1D* amplified), BT474 (*HER-2* amplified, *PPM1D* amplified), and ZR-75.30 (*HER-2* amplified, *PPM1D* amplified). *C,* cell survival in breast cancer cell lines after short hairpin RNA-mediated silencing of PPM1D expression using a previously validated pSUPER-PPM1D (24). Cells were transfected with either pSUPER-PPM1D or pSUPER-control and also a plasmid encoding blasticidin resistance. Blasticidin selection was initiated 48 h post-transfection and replenished every 3 days. After 14 days, viable cells were quantified using the sulforhodamine B colorimetric assay for cytotoxicity. Survival fraction is relative to the pSUPER-control. *D,* PPM1D inhibitor (CCT007093) 14-day sulforhodamine B colorimetric assay for cytotoxicity of 11 breast cancer cell lines with SF50 inhibitor concentrations (*right*). Cells harboring *PPM1D* gene amplification and mRNA overexpression (*red curves*) showed significantly increased sensitivity to CT007093 compared with cell lines lacking *PPM1D* gene amplification and overexpression (*black curves*).

in sporadic basal-like cancers may be similar to that observed in BRCA1 cancers and that these cancers may progress through similar genetic pathways. However, the pattern, type, and complexity of genetic changes are not only different between distinct molecular subgroups of breast cancer but also that within each group there is a significant degree of heterogeneity at the genetic level. For instance, luminal cancers were a mixture of "simplex," complex amplifier, and "sawtooth." It should be noted, however, that several recurrent genomic aberrations (loss of 8p, 11q, and 17p and gain of 3q, 5p, and 8q) were found in grade 3 IDC-NST regardless of the tumor phenotype. These regions, which have been shown to be rarely altered in grade 1 IDC-NST (10, 11), may be associated with the development of grade 3 breast cancers regardless of phenotype.

There has been controversy whether progression from grade 1 to 3 occurs in IDC-NST. Loss of the whole 16q arm has been shown to be preferentially found in grade 1 breast cancer (60-85% of cases versus 20-30% in grade 3 tumors; refs. 9–12) and has led to the hypothesis that progression from grade 1 to 3 cancers is an unlikely biological phenomenon. More recent studies have suggested, however, that a substantial proportion of grade 3 IDC-NST may stem from grade 1 breast cancers due to the accumulation of additional genetic changes (29, 30). In the present study, we observed a relatively low prevalence of 16q losses across all grade 3 IDC-NST, but 16q whole-arm loss was significantly more prevalent in grade 3 luminal (44%) when compared with nonluminal (22%) cancers ($P$ = 0.00494, Fisher's exact test). Based on these findings, we cannot rule out progression

from low-grade to high-grade IDC-NST, particularly in those of luminal phenotype.

Amplification of 17q23.2, including *PPM1D*, was found in 20% of HER-2 cancers and 8% of luminal tumors. Here, we show that *PPM1D* (*WIP1*) is consistently overexpressed when amplified in grade 3 IDC-NST. *PPM1D* encodes a member of the PPM serine/threonine phosphatase family, which has been shown to have oncogenic properties (24). PPM1D activation results in a negative regulation of p53 function and other tumor suppressor pathways most likely by selective inactivation of p38 kinase (39, 40). Furthermore, PPM1D also participates in the regulation of DNA repair via an interaction with UNG glycosylase (41), progesterone receptor function (42), and the regulation of CHK1, CHK2, and ATM kinases, which control DNA repair and cell cycle (43–47). PPM1D overexpression has been shown to recapitulate the antiapoptotic effects of *TP53* inactivating mutation *in vitro* and increases tumorigenicity in murine models *in vivo* (33, 34). Recent studies have shown that inactivation of p38 due to *PPM1D* gene amplification and expression contributes to the development of human cancers by suppressing p53 activation (34). As *PPM1D* mRNA expression levels were significantly higher in primary IDC-NST and breast cancer cell lines harboring *PPM1D* gene amplification, and this gene has been shown to be a candidate oncogene, we investigated whether the survival of luminal and *HER-2*-amplified cell line models harboring 17q23.2 gene amplification would be dependent on PPM1D signalling. We showed here that *PPM1D* silencing by a previously validated short hairpin RNA construct and the small-molecule inhibitor CCT007093 (24) is selectively lethal to cells harboring *PPM1D* amplification, indicating that the survival of cancer cells harboring 17q23.2 amplification is dependent on PPM1D expression and phosphatase activity. In contrast with previous reports (35, 48), however, our study suggests that *PPM1D* expression may be required for the survival of *PPM1D*-amplified cancer cells regardless of *TP53* status, given that BT474 cells harbor a *TP53* gene mutation (codon 285 G-to-A, Glu-to-Lys; ref. 49). This discrepancy may be explained by the fact that we used a long-term (14-day) cell viability assay rather than a short-term (5-day) assay described in previous reports (35, 48). Of interest, 37.5% of *PPM1D*-amplified primary tumors were positive for p53 expression by immunohistochemistry, which may suggest the presence of inactivating *TP53* mutations. Our findings suggest that *PPM1D* is one of the drivers of the 17q23.2 amplicon and that PPM1D is a possible therapeutic target for the subgroup of *PPM1D*-amplified luminal and HER-2 cancers.

Taken together, our results suggest that *PPM1D* gene amplification, like *HER-2* gene amplification, may constitute a predictive marker for future clinical and preclinical studies testing the efficacy of PPM1D inhibitors. Indeed, from a clinical perspective, apart from its prognostic value, which is often equivocal, the most important characteristic of any therapeutic target should be its value as a predictive marker for a specific therapy. For example, although the prognostic significance of *EGFR* amplification in non-small lung cell carcinoma remains controversial, its presence has nonetheless been significantly associated with improved disease control and survival outcome in patients with non-small lung cell carcinoma following combined treatment with the anti-epidermal growth factor receptor monoclonal antibody cetuximab and chemotherapy (50).

In conclusion, grade 3 IDC-NST constitute a heterogeneous group of tumors at the genetic level. Basal-like and HER-2 tumors, as defined by a classification system applicable to archival formalin-fixed material (3), preferentially display "sawtooth" and "firestorm" genetic patterns, respectively, and infrequently harbor 16q deletions, suggesting that the majority of these tumors are unlikely to evolve from grade 1 breast cancers. On the other hand, based on our data, we cannot rule out progression from grade 1 to 3 breast cancers in 20 of 45 (44%) of tumors of luminal phenotype. Amplification and overexpression of the *PPM1D* gene was found to be associated with luminal and HER-2 cancers. *In vitro* analysis suggests that PPM1D expression and phosphatase activity are required for the survival of breast cancer cells harboring amplification of 17q23.2. Hence, PPM1D may constitute a therapeutic target for luminal and HER-2 cancers harboring amplification of this gene. Our findings warrant further studies to define the functional significance of amplicons identified in this study in the respective molecular subtypes of breast cancer to which they pertain. Moreover, our results highlight the possibility of enriching the therapeutic armamentarium for the management of breast cancer patients by extending the functional classification of high-grade breast cancer beyond estrogen receptor and HER-2 status.

## Disclosure of Potential Conflicts of Interest

No potential conflicts of interest were disclosed.

## References


1. Perou CM, Sorlie T, Eisen MB, et al. Molecular portraits of human breast tumours. Nature 2000;406:747–52.
2. Hu Z, Fan C, Oh DS, et al. The molecular portraits of breast tumors are conserved across microarray platforms. BMC Genomics 2006;7:96.
3. Nielsen TO, Hsu FD, Jensen K, et al. Immunohistochemical and clinical characterization of the basal-like subtype of invasive breast carcinoma. Clin Cancer Res 2004;10:5367–74.
4. Cheang MC, Voduc D, Bajdik C, et al. Basal-like breast cancer defined by five biomarkers has superior prognostic value than triple-negative phenotype. Clin Cancer Res 2008;14:1368–76.
5. Tan DS, Marchio C, Jones RL, et al. Triple negative breast cancer: molecular profiling and prognostic impact in adjuvant anthracycline-treated patients. Breast Cancer Res Treat 2008;111:27–44.
6. Bergamaschi A, Kim YH, Wang P, et al. Distinct patterns of DNA copy number alteration are associated with different clinicopathological features and gene-expression subtypes of breast cancer. Genes Chromosomes Cancer 2006;45:1033–40.
7. Chin K, DeVries S, Fridlyand J, et al. Genomic and transcriptional aberrations linked to breast cancer pathophysiologies. Cancer Cell 2006;10:529–41.
8. Adelaide J, Finetti P, Bekhouche I, et al. Integrated profiling of basal and luminal breast cancers. Cancer Res 2007;67:11565–75.
9. Simpson PT, Reis-Filho JS, Gale T, Lakhani SR. Molecular evolution of breast cancer. J Pathol 2005;205:248–54.
10. Roylance R, Gorman P, Harris W, et al. Comparative genomic hybridization of breast tumors stratified by histological grade reveals new insights into the biological progression of breast cancer. Cancer Res 1999;59:1433–6.
11. Buerger H, Otterbach F, Simon R, et al. Comparative genomic hybridization of ductal carcinoma *in situ* of the breast-evidence of multiple genetic pathways. J Pathol 1999;187:396–402.
12. Buerger H, Schmidt H, Beckmann A, Zanker KS, Boecker W, Brandt B. Genetic characterisation of invasive breast cancer: a comparison of CGH and PCR

based multiplex microsatellite analysis. J Clin Pathol 2001;54:836–40.
13. Allred DC, Wu Y, Mao S, et al. Ductal carcinoma *in situ* and the emergence of diversity during breast cancer evolution. Clin Cancer Res 2008;14:370–78.
14. Nahta R, Esteva FJ. Trastuzumab: triumphs and tribulations. Oncogene 2007;26:3637–43.
15. Reis-Filho JS, Simpson PT, Turner NC, et al. FGFR1 emerges as a potential therapeutic target for lobular breast carcinomas. Clin Cancer Res 2006;12:6652–62.
16. Neve RM, Chin K, Fridlyand J, et al. A collection of breast cancer cell lines for the study of functionally distinct cancer subtypes. Cancer Cell 2006;10:515–27.
17. Marchio C, Iravani M, Natrajan R, et al. Genomic and immunophenotypical characterization of pure micropapillary carcinomas of the breast. J Pathol 2008; 215:398–410.
18. Coe BP, Ylstra B, Carvalho B, Meijer GA, Macaulay C, Lam WL. Resolving the resolution of array CGH. Genomics 2007;89:647–53.
19. Gunnarsson R, Staaf J, Jansson M, et al. Screening for copy-number alterations and loss of heterozygosity in chronic lymphocytic leukemia—a comparative study of four differently designed, high resolution microarray platforms. Genes Chromosomes Cancer 2008;47:697–711.
20. Natrajan R, Williams RD, Hing SN, et al. Array CGH profiling of favourable histology Wilms tumours reveals novel gains and losses associated with relapse. J Pathol 2006;210:49–58.
21. Hicks J, Krasnitz A, Lakshmi B, et al. Novel patterns of genome rearrangement and their association with survival in breast cancer. Genome Res 2006;16: 1465–79.
22. Lambros MB, Simpson PT, Jones C, et al. Unlocking pathology archives for molecular genetic studies: a reliable method to generate probes for chromogenic and fluorescent *in situ* hybridization. Lab Invest 2006;86: 398–408.
23. Arriola E, Marchio C, Tan DS, et al. Genomic analysis of the HER2/TOP2A amplicon in breast cancer and breast cancer cell lines. Lab Invest 2008;88: 491–503.
24. Rayter S, Elliott R, Travers J, et al. A chemical inhibitor of PPM1D that selectively kills cells overexpressing PPM1D. Oncogene 2008;27:1036–44.
25. Vichai V, Kirtikara K. Sulforhodamine B colorimetric assay for cytotoxicity screening. Nat Protoc 2006;1: 1112–6.
26. Reis-Filho JS, Drury S, Lambros MB, et al. ESR1 gene amplification in breast cancer: a common phenomenon? Nat Genet 2008;40:809–10; author reply 810–2.
27. Horlings HM, Bergamaschi A, Nordgard SH, et al. ESR1 gene amplification in breast cancer: a common phenomenon? Nat Genet 2008;40:807–8; author reply 810–2.
28. Brown LA, Hoog J, Chin SF, et al. ESR1 gene amplification in breast cancer: a common phenomenon? Nat Genet 2008;40:806–7; author reply 810–2.
29. Roylance R, Gorman P, PapiorT, et al. A comprehensive study of chromosome 16q in invasive ductal and lobular breast carcinoma using array CGH. Oncogene 2006;25:6544–53.
30. Korsching E, Packeisen J, Helms MW, et al. Deciphering a subgroup of breast carcinomas with putative progression of grade during carcinogenesis revealed by comparative genomic hybridisation (CGH) and immunohistochemistry. Br J Cancer 2004;90:1422–8.
31. Vincent-Salomon A, Gruel N, Lucchesi C, et al. Identification of typical medullary breast carcinoma as a genomic sub-group of basal-like carcinomas, a heterogeneous new molecular entity. Breast Cancer Res 2007;9:R24.
32. Sinclair CS, Rowley M, Naderi A, Couch FJ. The 17q23 amplicon and breast cancer. Breast Cancer Res Treat 2003;78:313–22.
33. Fuku T, Semba S, Yutori H, Yokozaki H. Increased wild-type p53-induced phosphatase 1 (Wip1 or PPM1D) expression correlated with downregulation of checkpoint kinase 2 in human gastric carcinoma. Pathol Int 2007;57:566–71.
34. Castellino RC, De Bortoli M, Lu X, et al. Medulloblastomas overexpress the p53-inactivating oncogene WIP1/PPM1D. J Neurooncol 2008;86:245–56.
35. Parssinen J, Alarmo EL, Karhu R, Kallioniemi A. PPM1D silencing by RNA interference inhibits proliferation and induces apoptosis in breast cancer cell lines with wild-type p53. Cancer Genet Cytogenet 2008; 182:33–9.
36. Jonsson G, Naylor TL, Vallon-Christersson J, et al. Distinct genomic profiles in hereditary breast tumors identified by array-based comparative genomic hybridization. Cancer Res 2005;65:7612–21.
37. Turner NC, Reis-Filho JS. Basal-like breast cancer and the BRCA1 phenotype. Oncogene 2006;25: 5846–53.
38. Melchor L, Honrado E, Huang J, et al. Estrogen receptor status could modulate the genomic pattern in familial and sporadic breast cancer. Clin Cancer Res 2007;13:7305–13.
39. Fiscella M, Zhang H, Fan S, et al. Wip1, a novel human protein phosphatase that is induced in response to ionizing radiation in a p53-dependent manner. Proc Natl Acad Sci U S A 1997;94:6048–53.
40. Bulavin DV, Phillips C, Nannenga B, et al. Inactivation of the Wip1 phosphatase inhibits mammary tumorigenesis through p38 MAPK-mediated activation of the p16 (Ink4a)-p19 (Arf) pathway. Nat Genet 2004;36:343–50.
41. Lu X, Bocangel D, Nannenga B, Yamaguchi H, Appella E, Donehower LA. The p53-induced oncogenic phosphatase PPM1D interacts with uracil DNA glycosylase and suppresses base excision repair. Mol Cell 2004;15:621–34.
42. Proia DA, Nannenga BW, Donehower LA, Weigel NL. Dual roles for the phosphatase PPM1D in regulating progesterone receptor function. J Biol Chem 2006;281:7089–101.
43. Lu X, Nannenga B, Donehower LA. PPM1D dephosphorylates Chk1 and p53 and abrogates cell cycle checkpoints. Genes Dev 2005;19:1162–74.
44. Fujimoto H, Onishi N, Kato N, et al. Regulation of the antioncogenic Chk2 kinase by the oncogenic Wip1 phosphatase. Cell Death Differ 2006;13: 1170–80.
45. Nannenga B, Lu X, Dumble M, et al. Augmented cancer resistance and DNA damage response phenotypes in PPM1D null mice. Mol Carcinog 2006;45: 594–604.
46. Yu E, Ahn YS, Jang SJ, et al. Overexpression of the wip1 gene abrogates the p38 MAPK/p53/Wip1 pathway and silences p16 expression in human breast cancers. Breast Cancer Res Treat 2007;101: 269–78.
47. Shreeram S, Hee WK, Demidov ON, et al. Regulation of ATM/p53-dependent suppression of myc-induced lymphomas by Wip1 phosphatase. J Exp Med 2006; 203:2793–9.
48. Parssinen J, Alarmo EL, Khan S, Karhu R, Vihinen M, Kallioniemi A. Identification of differentially expressed genes after PPM1D silencing in breast cancer. Cancer Lett 2008;259:61–70.
49. Concin N, Zeillinger C, Tong D, et al. Comparison of p53 mutational status with mRNA and protein expression in a panel of 24 human breast carcinoma cell lines. Breast Cancer Res Treat 2003;79:37–46.
50. Hirsch FR, Herbst RS, Olsen C, et al. Increased EGFR gene copy number detected by fluorescent *in situ* hybridization predicts outcome in non-small-cell lung cancer patients treated with cetuximab and chemotherapy. J Clin Oncol 2008;26:3351–7.

Clinical Cancer Research

# Tiling Path Genomic Profiling of Grade 3 Invasive Ductal Breast Cancers

Rachael Natrajan, Maryou B. Lambros, Socorro María Rodríguez-Pinilla, et al.

*Clin Cancer Res* 2009;15:2711-2722.